

Application of the Wheeler Incremental Inductance Rule for Robust Design and Modeling of MMIC Spiral Inductors

Grant A. Ellis

Department of Electrical and Electronic Engineering
Universiti Teknologi Petronas, 31750 Tronoh, Perak Darul Ridzuan, Malaysia
grant_ellis@petronas.com.my

Abstract — A physics based model using Wheelers incremental inductance rule for calculating the change in inductance due to variations in line width and thickness for planar circular spiral inductors is given. It is shown that the series resistance of an MMIC inductor can be used as a figure of merit for the robustness of the inductor against etching variations in line width during fabrication. Circular inductors are shown to have less inductance variation than rectangular inductors. This model can be evaluated quickly using a circuit simulator without the need for expensive EM analysis. In the electromagnetic modeling of MMIC inductors, a fine grid and several sheets are used to accurately model the current distribution and determine the resistance. Sonnet™ is used to accurately model the 3D characteristics of thick conductors such as loss and effects of physically thick metal. A procedure based on the Richardson extrapolation method is used to extract the resistance values without long computation time. Applications include calculating the change in inductance due to over- or under-etching of metal lines during fabrication. For 2 to 4 turn inductors with variations in line width of +/-20% of the nominal width, the average variation in modeled inductance is within 8% of the EM simulated variation.

Index Terms - Microwave components, MMIC technology, planar inductors.

I. INTRODUCTION

During fabrication of the MMIC inductors, variations in line width or line thickness may occur. This can be due to variations in the etch

rates during wafer processing. The effect of these processing variations can result in the detuning of the MMICs lowering circuit yield. As development cycles for wireless products accelerate, design techniques for planar spiral inductors for robust performance in the presence of these process variations in the fabrication of MMICs become necessary.

In design and optimization of microwave circuits using planar spiral inductors, extensive use is made of equivalent circuit models like the one shown in Fig. 1. The circuit parameters, L_0 , $R(f)$, C , and $C_{g1,2}$ are specified for a given number of turns, line width, and center-to-center line spacing.

Electromagnetic (EM) simulation is necessary in modeling planar inductors due to their complex structure and effects such as skin and proximity effects between the conductors and mutual inductance between the turns. Full-wave EM simulation of planar inductors can be expensive in terms of computation time and memory, making calculation of circuit response, and circuit yield prohibitive.

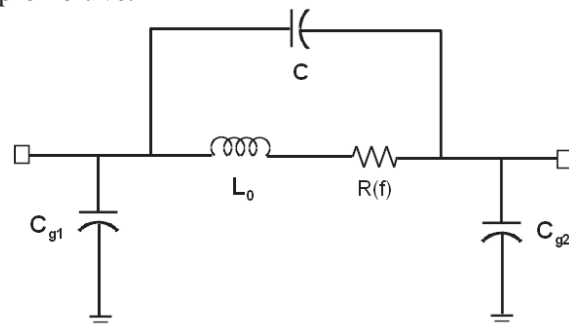


Fig. 1. Equivalent nominal circuit model for spiral inductor used in MMICs.

The Wheeler incremental inductance rule shows that the total change in inductance due to the variation of all conductor surfaces is proportional to the resistance [1-5]. In our earlier paper [6], the inductance change due to variation in the width and thickness of the inductor line was approximated for circular inductors. Here, circular inductors are assumed to have a nearly continuous current distribution while rectangular inductors due to current crowding in the corners have a mostly discontinuous distribution.

The incremental inductance rule allows for the determination of the high frequency resistance of an electrical conductor from its external inductance. A typical application of the incremental inductance rule is for calculating the resistance and loss of a conductor based on information about its inductance [2]. In this paper, the incremental inductance rule is used in reverse of the conventional approach to calculate the change in inductance given its known nominal resistance and assuming variation in one of the physical parameters, namely its conductor width, w , or thickness, t .

The incremental inductance rule can be used to quickly estimate the variation in inductance due to variation in the conductor line width or thickness given only its nominal resistance value. The estimate for variation in inductance together with the known nominal inductance can be used to calculate the total inductance due to over- or under-etching of the metal lines.

Sonnet em [7] is a method of moments based analysis tool and is used to calculate the scattering parameters for several inductors. The resulting equivalent circuit model parameters are extracted and the series resistance values are used to estimate the change in inductance due to variation in line width. Using this method, accurate calculation of the resistance becomes necessary. Multiple sheets and a fine discretization grid must be used to get high accuracy. A convergence test is used to verify the extracted model parameter values. An alternative to the method of moments is a stochastic solution for extraction of external inductances [8]. The advantage of the stochastic methodology is that it requires no discretization or meshing.

This paper is organized as follows: Section II describes the Wheeler incremental inductance rule

and a simple model is derived for the normalized change in inductance for microstrip lines; Section III the model is verified; Section IV gives results for the change in inductance for different inductors; and finally, the paper is concluded.

II. THEORETICAL DEVELOPMENT

The Wheeler incremental inductance rule states that the high frequency loss resistance of a conductor can be determined from the normal derivative of its inductance. This rule applies to all conductor shapes for which the current flow is determined by the skin effect. This rule assumes that the radius of curvature of each conductor is large compared with the conductor skin depth (preferably several skin depths) [2]. For a rectangular microstrip line, the incremental inductance rule becomes (see Fig. 2a and 2b):

$$R(f) = \frac{R_s}{\mu_0} \sum_{j=1}^6 \frac{\partial L}{\partial n_j} = \frac{R_s}{\mu_0} \left(-2 \frac{\partial L}{\partial w} - 2 \frac{\partial L}{\partial t} + 2 \frac{\partial L}{\partial h} \right), \quad (1)$$

where $R_s = \sqrt{\pi f \mu / \sigma}$ is the surface resistance of the conductor and n_j is the normal pointing into the j^{th} conductor surface.

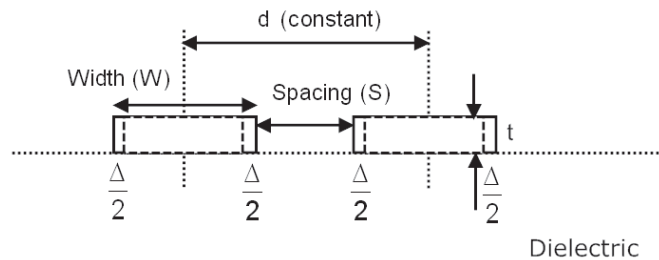


Fig. 2a. Cross-section of microstrip lines showing under-etch/over-etch of lines.

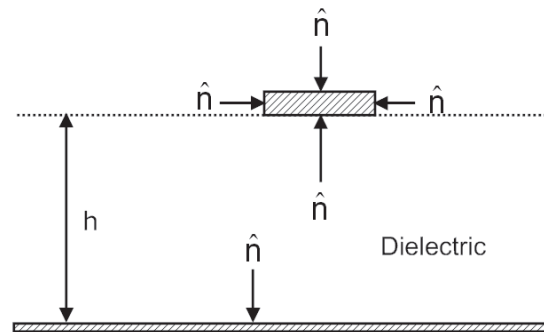


Fig. 2b. Cross-section of microstrip line showing normal vector to each conducting surface.

A widely used expression for microstrip line inductance is from Wheeler [2]:

$$L = \frac{\mu_0}{2\pi} l \left[\ln \left(\frac{8h}{w'} \right) + \frac{l}{32} \left(\frac{w'}{h} \right)^2 + \dots \right], \quad (2)$$

for $w'/h \leq 1$ and w' is the equivalent conductor width and l is the length of the microstrip line.

Microstrip transmission lines having width w and nonzero thickness ($t > 0$) can be modeled as a conductor having zero thickness ($t = 0$) and an equivalent conductor width given by $w' = w + \Delta w$. Different widths (Δw) must be used depending on the transmission line parameter being considered e.g. L , C , Z_0 , or ϵ_{eff} [3]. The inductance (L) is not affected by the substrate dielectric constant. For microstrip, an accurate model for the increment in the conductor width is given by [9] and the equivalent line width becomes:

$$w' = w + \Delta w = w + \frac{t}{\pi} \left(1 + \ln \left(\frac{4\pi w}{t} \right) \right). \quad (3)$$

Using the above definition for L , the ratio of the incremental inductance from one side of the microstrip to the total incremental inductance is approximated for $h \gg w$ as:

$$C(h, w, t) = \frac{-\partial L / \partial w}{\sum_j \frac{\partial L}{\partial n_j}} \approx \frac{1 + t / (\pi w)}{2 + 2t / (\pi w) + \frac{2}{\pi} \ln \left(\frac{4\pi w}{t} \right) + \frac{2w'}{h}}. \quad (4a)$$

The ratio of the change in incremental inductance from the top of the microstrip line to the total incremental inductance can be approximated as:

$$D(h, w, t) = \frac{-\partial L / \partial t}{\sum_j \frac{\partial L}{\partial n_j}} \approx \frac{\frac{1}{\pi} \ln \left(\frac{4\pi w}{t} \right)}{2 + 2t / (\pi w) + \frac{2}{\pi} \ln \left(\frac{4\pi w}{t} \right) + \frac{2w'}{h}}. \quad (4b)$$

Substituting the partial change in inductance in equations (4a) and (4b) into the definition for loss resistance in equation (1), the change in inductance verse change in line width for the microstrip is:

$$\frac{dL}{dw} = C(h, w, t) \frac{\mu_0}{R_s} R(f), \quad (5a)$$

and the change in inductance verse change in line thickness becomes:

$$\frac{dL}{dt} = D(h, w, t) \frac{\mu_0}{R_s} R(f). \quad (5b)$$

III. MODEL VERIFICATION

To corroborate the above, $C(h, w, t)$ and $D(h, w, t)$ are compared with the simulated change in inductance for a microstrip line using Sonnet. Sonnet is a full wave electromagnetic simulator for planar microwave structures and is a tool of choice due to high accuracy requirements. Microstrip lines with length $l = 150 \mu\text{m}$ and width varying from 3 to 20 μm on Gallium Arsenide (GaAs, $\epsilon_r = 12.9$) with a substrate thickness of $h = 100 \mu\text{m}$ and metal thickness of $t = 2 \mu\text{m}$ are simulated. The microstrip conductor is Gold and for simplicity the loss tangent for the GaAs substrate is assumed to be zero. The thick metal approximation in Sonnet is used to accurately model the 3D characteristics of thick conductors such as loss and electromagnetic effects of physically thick metal such as coupling between closely spaced conductors.

For accurate EM analysis, a calibration procedure is first carried out to determine the number of sheets and grid spacing necessary. The microstrip line with $w = 5 \mu\text{m}$ and $10 \mu\text{m}$ is analyzed for increasing the number of sheets and different grid spacing. The number of sheets is increased until the extracted resistance and inductance values of the microstrip line converge [10]. The pointer robust optimization in Microwave Office is used to extract the series inductance, resistance, and shunt capacitance to ground [11]. This optimization uses multiple search methods to fit the simulated data from Sonnet to the microstrip equivalent circuit model. At 16 GHz, the $t = 2 \mu\text{m}$ thick Gold microstrip line is about 3 skin depths thick. The extracted

inductance value is nearly independent of the number of sheets. For $w = 5 \mu\text{m}$, the extracted resistance value converges for 15 sheets using a $0.5 \mu\text{m}$ grid. For $w = 10 \mu\text{m}$, the extracted resistance value converges to within 5% of the final value for 20 sheets using a $1 \mu\text{m}$ grid.

To conserve simulation time, a $0.5 \mu\text{m}$ layout grid is used for $5 \mu\text{m}$ wide lines, and a $1 \mu\text{m}$ grid is used for $10 \mu\text{m}$ wide lines. Also, 20 sheets or about five sheets per skin depth at 16 GHz are used to model the thick conductor. Using the extracted values for $R(f)$ and L for the microstrip line at $f = 16 \text{ GHz}$, $\sum_j \partial L / \partial n_j$ is calculated using (1), and $\partial L / \partial w$ and $\partial L / \partial t$ are approximated by calculating $\Delta L / \Delta w$ and $\Delta L / \Delta t$ for $w = 3 - 20 \mu\text{m}$. Figure 3 shows the ratio of the change in inductance due to recession of the line width and line thickness versus the total change in inductance caused by recession of all conductor surfaces using the models $C(h,w,t)$ and $D(h,w,t)$, and the extracted EM values for $\frac{-\partial L / \partial t}{\sum_j \partial L / \partial n_j}$ and

$$\frac{-\partial L / \partial t}{\sum_j \partial L / \partial n_j}$$

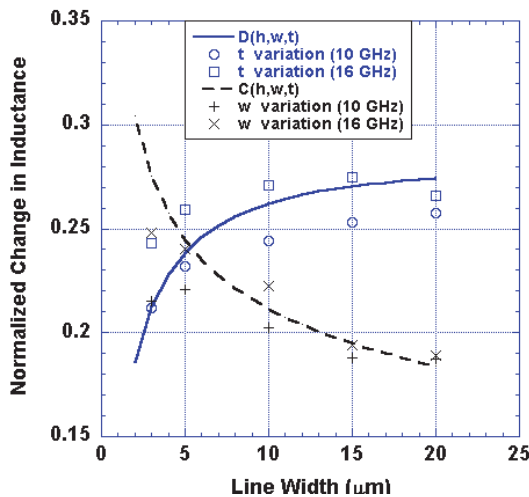


Fig. 3. Ratio of change in inductance due to change in line width and thickness vs. change in total inductance for $t = 2 \mu\text{m}$ line.

These models agree quite well with the extracted values for $f = 16 \text{ GHz}$ and $w \geq 5 \mu\text{m}$. The modeled and extracted values for normalized

changes in inductance for $f = 10 \text{ GHz}$ begin to diverge for $w < 5 \mu\text{m}$. At 10 GHz, the skin depth for Gold is $0.8 \mu\text{m}$.

Circular inductors on GaAs substrates plated up to $9 \mu\text{m}$ metal thickness have been reported [12]. In most cases, circular spiral inductors have higher Q and lower resistance than rectangular inductors [12]. The higher resistance in the rectangular inductors is mainly due to the resistance in the corners that are not present in circular inductors. At high frequencies, currents crowd inside of the inner bends and result in higher resistance. The incremental inductance rule implies that the lower resistance in circular inductors results in circular inductors having less variation in inductance than rectangular inductors due to variations in cross section. Circular inductors have no corners and result in more uniform current distribution along the length of the inductor. Figures 4a and 4b show the magnitude of the computed current density using Sonnet for rectangular and circular inductors at 16 GHz. EM simulations were carried out with Sonnet, Release 12 [7] on a workstation using a dual Intel Xeon 2.66 GHz CPU (8 cores) and 16 GByte of RAM. In the next section, simulation results show that circular inductors have lower resistance than the corresponding rectangular inductors with nearly the same dimensions and inductance values.

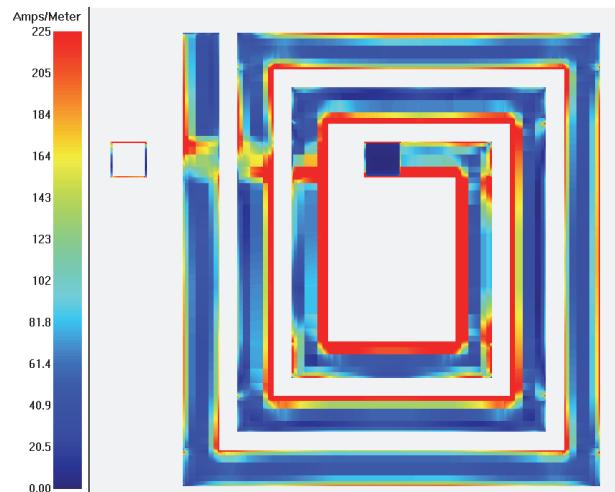


Fig. 4a. Current distribution for three-turn rectangular inductor with $w = 10 \mu\text{m}$ and $s = 5 \mu\text{m}$ at 16 GHz.

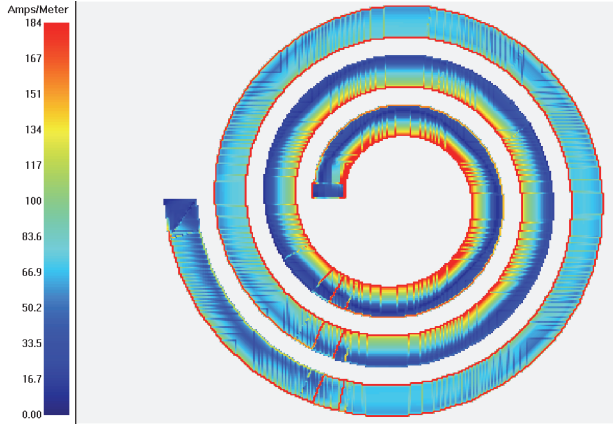


Fig. 4b. Current distribution for three-turn circular inductor with $w = 10 \mu\text{m}$ and $s = 5 \mu\text{m}$ at 16 GHz.

IV. RESULTS

A. Change in inductance

The total inductance including variation due to change in line width Δw and thickness Δt are modeled to first order as:

$$L \cong L_0 + \frac{dL}{dw} \Delta w, \text{ and} \quad (6a)$$

$$L \cong L_0 + \frac{dL}{dt} \Delta t, \quad (6b)$$

where L_0 is the nominal inductance (no over- or under-etch) and dL/dw and dL/dt are computed using (6a) and (6b).

Microstrip inductors with line width, $w = 5$ and $10 \mu\text{m}$ and spacing, $s = 5 \mu\text{m}$ on Gallium Arsenide (GaAs, $\epsilon_r = 12.9$) with a substrate thickness of $h = 100 \mu\text{m}$ and metal thickness of $t = 2 \mu\text{m}$ are simulated. The microstrip conductor is Gold and for simplicity the loss tangent for the GaAs substrate is assumed to be zero. The thick metal approximation in Sonnet is used to accurately model the 3D characteristics of thick conductors such as loss and electromagnetic effects of physically thick metal such as coupling between closely spaced conductors. For circular inductors, a conformal type mesh is used. For rectangular inductors, the staircase type fill is used.

Circular spiral inductors with $N = 2$ to 4 turns and nominal line widths of $5 \mu\text{m}$ and $10 \mu\text{m}$ are considered. The nominal spacing is $5 \mu\text{m}$. The center-to-center line spacing is held constant and

the line thickness is fixed at $t = 2 \mu\text{m}$. For the first case, all line widths except for the airbridge are under etched and over etched 1 and $2 \mu\text{m}$. For the second case, the line width and spacing are fixed at the nominal values and the line thickness is under etched and over etched $0.5 \mu\text{m}$ and $1 \mu\text{m}$ from the nominal line thickness $t = 2 \mu\text{m}$.

Using the procedure described earlier, the simulated data for the circular inductors from Sonnet are fit to the equivalent circuit model in Fig. 1 at $f = 16$ GHz. Figures 5a and 5b show the modeled inductance using equation (6a) and extracted inductance vs. amount of over- and under-etching of line width, Δw . Figures 6a and 6b show the modeled inductance using equation (6b) and extracted inductance vs. amount of over- and under-etching of line thickness, Δt . The extracted inductances vary linearly with Δw and Δt [13-14].

Tables 1a and 1b show the variation in inductance between the models in equations (6a) and (6b) and the extracted values from EM simulation. For $N = 3$ turns and $w = 5 \mu\text{m}$, the variation in extracted inductance due to variation in line width is 13 %. For $N = 3$ turns and $w = 10 \mu\text{m}$, the variation in extracted inductance is 10.8 %. These values compare well with the modeled inductance variations of 14 % and 10 %. For $N = 3$ turns and $w = 5 \mu\text{m}$, the variation in extracted inductance due to variation in line thickness is 6.6 %. For $N = 3$ turns and $w = 10 \mu\text{m}$, the variation in extracted inductance is 6.2 %. These values compare well with the modeled inductance variations of 6.8 % and 6.2 %.

B. Circular vs. rectangular inductors

The equivalent circuit model parameters are now computed for circular and rectangular planar inductors. The resistance for circular and rectangular inductors having nearly the same inductance will be extracted and the relationship between the resistance and change in inductance will be shown [14]. The microstrip inductors with $N = 3$ and 4 turns are analyzed for increasing number of sheets and finer grid spacing. For accurate EM analysis, the procedure used in the previous section is modified to minimize computation time by extrapolating the resistance value.

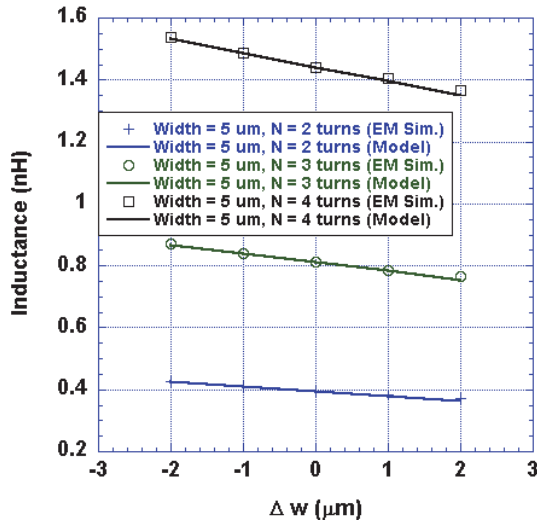


Fig. 5a. Inductance vs. Δw for $w = 5 \mu\text{m}$.

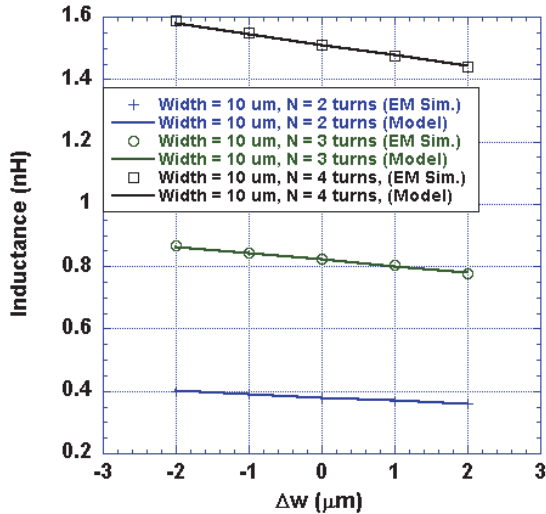


Fig. 5b. Inductance vs. Δw for $w = 10 \mu\text{m}$.

Using the earlier work by Richardson [15-17], a more accurate solution is achieved without a very fine discretization. A convergence ratio gives a measure of the goodness of the extrapolation. For true monotonic convergence, the convergence ratio is unity. Tables 2a-b and 3a-b show the extracted resistance, inductance, and parallel capacitance values of two circular inductors having $w = 10 \mu\text{m}$ and $N = 3$ and 4 turns. The extrapolated values using the 3-point Richardson's extrapolation technique are included. As shown in these Tables, the inductance and parallel capacitance values converge very quickly. The resistance values, however, converge more

slowly. The extracted resistance and inductance values converge to within 1 % of their final value for 15 sheets using a $0.5 \mu\text{m}$ grid. To conserve simulation time, a $0.5\text{-}\mu\text{m}$ minimum layout grid size is used for $10 \mu\text{m}$ wide lines. Also, 15 sheets or about five sheets per skin depth at 16 GHz are used to model the thick conductor.

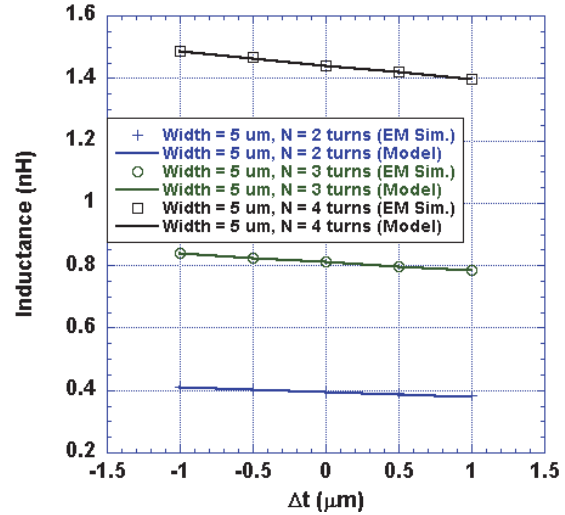


Fig. 6a. Inductance vs. Δt for $w = 5 \mu\text{m}$.

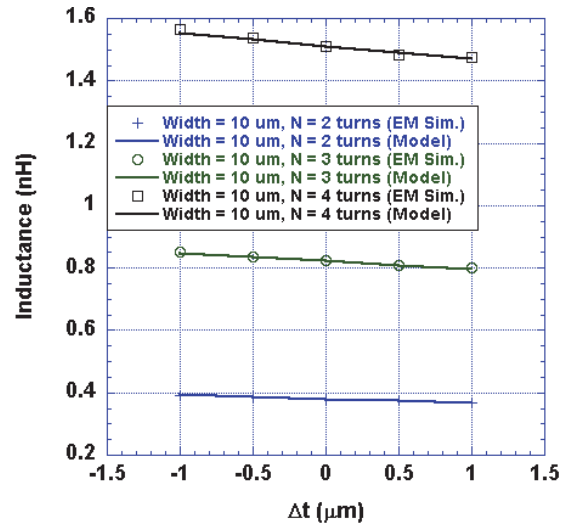


Fig. 6b. Inductance vs. Δt for $w = 10 \mu\text{m}$.

Using the procedure described above, the simulated data for four circular and rectangular inductors from Sonnet are used to extract the equivalent inductance and resistance values versus variation in line width, Δw at $f = 16 \text{ GHz}$. The inductors have $N = 3$ and 4 turns, with $w = 5$ and $10 \mu\text{m}$ and $s = 5 \mu\text{m}$. The rectangular and circular

inductors also have nearly the same nominal inductance value, e.g. 0.81 nH for $N = 3$ turns, $w = 5 \mu\text{m}$ and 1.45 nH for $N = 4$ turns, $w = 5 \mu\text{m}$. Figures 7a and 7b show the extracted resistance and inductance values vs. over- and under-etch of the line width, Δw for $N = 3$ turns, $w = 5$ and $10 \mu\text{m}$. Figures 7c and 7d show the extracted resistance and inductance values vs. amount of over- and under-etch of the line width, Δw for $N = 4$ turns, $w = 5$ and $10 \mu\text{m}$. In each case, the center line to line spacing, $w + s$, is held constant and the extracted inductance values vary linearly with Δw . The nominal resistance vs. the total change in inductance for the circular and rectangular inductors is shown in Table 4. For $N = 3$ turns and $w = 10 \mu\text{m}$, the variation in extracted inductance due to variation in line width is $\pm 10.7\%$ for the rectangular inductor and $\pm 5.5\%$ for the circular inductor. For $N = 4$ turns and $w = 10 \mu\text{m}$, the variation in extracted inductance due to variation in line width is $\pm 9.5\%$ for the rectangular inductor and only $\pm 5\%$ for the circular inductor.

Table 1a: Variation in inductance for $\Delta w = \pm 2 \mu\text{m}$

Inductor	EM Simulation	Model using (6a)
$N = 2, w = 5 \mu\text{m}$	13.5 %	15.3 %
$N = 2, w = 10 \mu\text{m}$	10.2 %	10.6 %
$N = 3, w = 5 \mu\text{m}$	13 %	14 %
$N = 3, w = 10 \mu\text{m}$	10.8 %	10 %
$N = 4, w = 5 \mu\text{m}$	11.8 %	12.6 %
$N = 4, w = 10 \mu\text{m}$	9.7 %	9 %

Table 1b: Variation in inductance for $\Delta t = \pm 1 \mu\text{m}$

Inductor	EM Simulation	Model using (6b)
$N = 2, w = 5 \mu\text{m}$	7.2 %	7.5 %
$N = 2, w = 10 \mu\text{m}$	6.4 %	6.6 %
$N = 3, w = 5 \mu\text{m}$	6.6 %	6.8 %
$N = 3, w = 10 \mu\text{m}$	6.2 %	6.2 %
$N = 4, w = 5 \mu\text{m}$	6.3 %	6.1 %
$N = 4, w = 10 \mu\text{m}$	6.1 %	5.6 %

Table 2a: Convergence ratio (CR) for circular inductor resistance ($w = 10 \mu\text{m}, N = 4$ turns)

Grid / # sheets	1 μm (10)	0.714 μm (14)	0.5 μm (20)	Extrap-olated Value	CR
10	5.02 Ω	5.37 Ω	5.64 Ω	5.96 Ω	0.98
15	5.03 Ω	5.45 Ω	5.75 Ω	6.01 Ω	0.99
20	5.03 Ω	5.5 Ω	5.78 Ω	6.08 Ω	0.99

Table 2b: Extracted inductance and parallel capacitance values for circular inductor ($w = 10 \mu\text{m}, N = 4$ turns)

Grid / # sheets	1 μm (10)	0.714 μm (14)	0.5 μm (20)
10	1.512 nH 0.014 pF	1.511 nH 0.0141 pF	1.515 nH 0.0141 pF
15	1.512 nH 0.0141 pF	1.511 nH 0.0141 pF	1.515 nH 0.0142 pF
20	1.512 nH 0.0141 pF	1.513 nH 0.0141 pF	1.516 nH 0.0142 pF

Table 3a: Convergence ratio (CR) for circular inductor resistance ($w = 10 \mu\text{m}, N = 3$ turns)

Grid / # sheets	1 μm (10)	0.714 μm (14)	0.5 μm (20)	Extrap-olated Value	CR
10	2.96 Ω	3.17 Ω	3.33 Ω	3.51 Ω	0.99
15	3.0 Ω	3.23 Ω	3.41 Ω	3.61 Ω	0.99
20	3.03 Ω	3.24 Ω	3.43 Ω	3.65 Ω	0.98

Table 3b: Extracted inductance and parallel capacitance values for circular inductor ($w = 10 \mu\text{m}, N = 3$ turns)

Grid / # sheets	1 μm (10)	0.714 μm (14)	0.5 μm (20)
10	0.8237 nH 0.0113 pF	0.8223 nH 0.0113 pF	0.8249 nH 0.0113 pF
15	0.8244 nH 0.0116 pF	0.8227 nH 0.0113 pF	0.8246 nH 0.0114 pF
20	0.8246 nH 0.0114 pF	0.8233 nH 0.0113 pF	0.8253 nH 0.0113 pF

Table 4: Resistance vs. change in inductance

	R Circular	R Rectangular	ΔL Circular	ΔL Rectangular
$N=3, w=5\mu\text{m}$	3.5Ω	4.8Ω	$\pm 6.4\%$	$\pm 13\%$
$N=4, w=5\mu\text{m}$	5.8Ω	7.8Ω	$\pm 5.3\%$	$\pm 7\%$
$N=3, w=10\mu\text{m}$	3.6Ω	4.4Ω	$\pm 5.5\%$	$\pm 10.7\%$
$N=4, w=10\mu\text{m}$	6.1Ω	7.8Ω	$\pm 5\%$	$\pm 9.5\%$

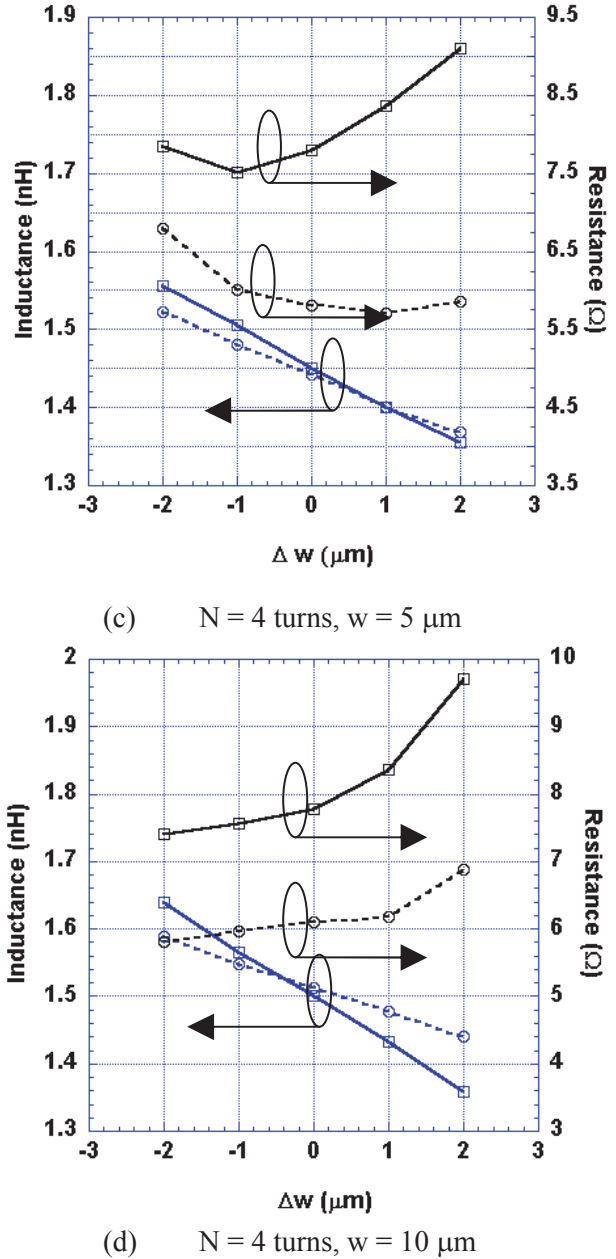
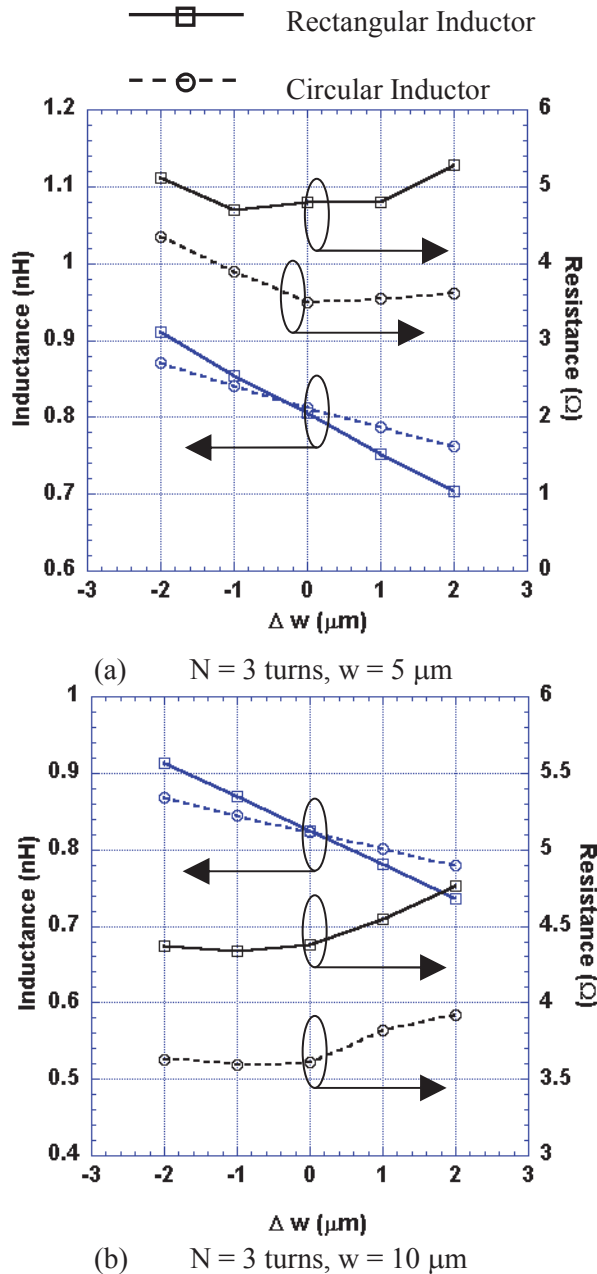


Fig. 7. Variation in Inductance and Resistance vs. over- and under-etch.

V. DISCUSSION

In the proceeding section, the optimum line width for minimum resistance can be seen as a tradeoff between the resistance of the line and the resistance due to proximity effect between adjacent lines. The close proximity of the lines and the resulting magnetic fields due to the currents flowing in them redistributes the currents causing higher resistance. Consider parallel round

wires having currents flowing in the same direction. This is similar to the case for planar inductors. Each wire has radius a , and the center-to-center spacing is $2b$.

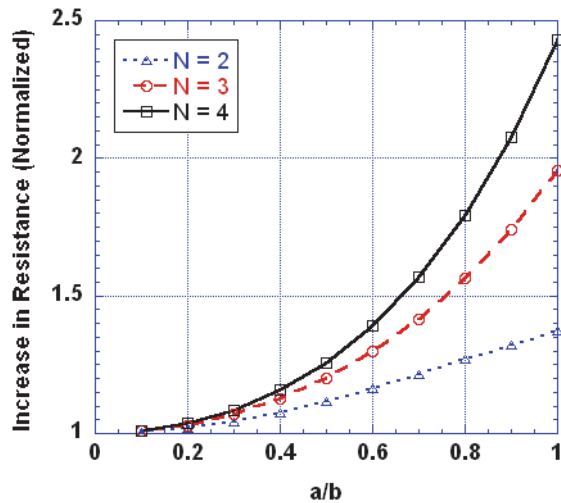


Fig. 8. Proximity effect in parallel conductors.

For small a/b , the increase in proximity resistance is negligible. As the diameter of the wires increases and approaches the spacing, the proximity resistance increases [18]. For more than two wires ($N > 2$) the increase in resistance becomes even greater (Fig. 8).

VI. CONCLUSION

The variation in inductance for circular planar spiral inductors due to variation in line width and thickness using the Wheeler incremental inductance rule has been investigated. The extracted inductance and capacitance values for planar microstrip inductors using electromagnetic analysis are shown to converge quickly requiring only a $1 \mu\text{m}$ grid and a few sheets. The extracted resistance values are shown to converge more slowly. At least a $0.5 \mu\text{m}$ grid and up to five sheets per skin depth are required to accurately capture the cross sectional current distribution of the conductor. An extrapolation procedure is used to accurately extract the resistance values to minimize computation time. The agreement between the modeled and EM simulated variation in inductance is good. This technique can be implemented quickly using a circuit simulator without the need for expensive EM analysis. Results show that circular inductors are more

tolerant than rectangular inductors to variations in line width as anticipated by the Wheeler incremental inductance rule. Circular inductors show about one half of the variation in the inductance value due to over- or under-etching than corresponding rectangular inductors having the same inductance value. The results show that an optimum line width can be found for minimum resistance in planar spiral inductors.

ACKNOWLEDGEMENTS

The author wishes to thank Sonnet Software and Applied Wave Research for their generous support.

REFERENCES

- [1] H. A. Wheeler, "Formulas for the Skin Effect," *Proc. IRE*, vol. 30, no. 9, pp. 412-424, Sept. 1942.
- [2] R. A. Pucel, D. J. Masse, and C. P. Hartwig, "Losses in Microstrip," *IEEE Trans. Microw. Theory Tech.*, vol. 16, no. 6, pp.342-350, June 1968.
- [3] R. K. Hoffmann, *Handbook of Microwave Integrated Circuits*, Boston, Artech House, 1987.
- [4] G. Kompa, *Practical Microstrip Design and Applications*, Boston, Artech House, 2005.
- [5] L. Dworsky, *Modern Transmission Line Theory and Applications*, New York, Wiley, 1979.
- [6] G. A. Ellis, "Application of Wheeler's Incremental Inductance Rule for Simulating the Effect of Etching Variations in Circular Inductors in MMICs," *INAS 2009*, Dec. 2009.
- [7] Sonnet Suites, Release 12, "Users Guide", Chapter 18, Syracuse NY, 2009.
- [8] K. Chatterjee, "A Stochastic Algorithm for the Extraction of Partial Inductances in IC Interconnect Structures," *Applied Computational Electromagnetic Society (ACES) Journal*, vol. 21, no. 1, pp. 81-89, March 2006.
- [9] H. A. Wheeler, "Transmission-Line Properties of Parallel Strips Separated by a Dielectric Sheet," *IEEE Microw. Theory Tech*, vol. 13, no. 3, pp. 172-185, March 1965.
- [10] D. L. Sanderson, J. C. Rautio, R. A. Groves, and S. Raman, "Accurate Modeling of Monolithic Inductors using Conformal

- Meshing for Reduced Computation,” *IEEE Micro. Mag.*, pp. 87-96, Dec. 2003.
- [11] Microwave Offices 2008, AWR, MWO/AO User’s Guide.
- [12] I. J. Bahl, “High Performance Inductors,” *IEEE Trans. Microw. Theory Tech.*, vol. 49, no. 4, pp. 654-664, April 2001.
- [13] S. Abdelbagi and G. A. Ellis, “Effects of Variations in Line Width on the Equivalent Circuit Model of Microstrip Spiral Inductors Implemented using GaAs Technology,” *SCORED 2008*, pp. 267-1–267-4, Nov. 2008.
- [14] G. A. Ellis, “Application of the Wheeler Incremental Inductance Rule for Robust Design and Modeling of MMIC Spiral Inductors,” *26th Annual Review of Progress in Applied Computational Electromagnetics*, Tampere, Finland, April 26-29, 2010.
- [15] R. C. Culver, “The Use of Extrapolation Techniques with Electrical Network Analogue Solutions,” *Brit J. Appl. Phys.*, vol. 3, pp. 376-378, 1952.
- [16] H. E. Green, “The Numerical Solution of Some Important Transmission Line Problems,” *IEEE Trans. Microw. Theory Tech*, vol. MTT-13, no. 5, pp. 676-692, 1965.
- [17] R. Garg, *Analytical and Computational Methods in Electromagnetics*, Boston, Artech House, 2008.
- [18] S. Butterworth, “On the Alternating Current Resistance of Solenoidal Coils”, *Proc. Roy. Soc.* vol. 107A, p. 693, 1925.



Grant A. Ellis received his Ph.D. degree in Electrical Engineering from the University of Washington, Seattle, in 1995. He is currently Professor of Electrical and Electronic Engineering at the Universiti Teknologi Petronas in Tronoh, Malaysia. His research interests are Monolithic Microwave Integrated Circuit (MMIC) and RFIC design, Microwave computer aided design techniques, and radiowave propagation analysis. Dr. Ellis is the founding chairman of the IEEE MTT/ED/AP Penang Chapter. He has been a Senior Member of the IEEE since 2004.